Surveying the Epsilon Eridani system Using MagAO

Surveying the Epsilon Eridani system Using MagAO

Rachel E. Morgan, Ewan S. Douglas, Kerri L. Cahoy, Jared R. Males, Katie M. Morzinski, et al.

Rachel E. Morgan, Ewan S. Douglas, Kerri L. Cahoy, Jared R. Males, Katie M. Morzinski, Laird Close, "Surveying the Epsilon Eridani system Using MagAO," Proc. SPIE 10703, Adaptive Optics Systems VI, 107032M (10 July 2018); doi: 10.1117/12.2313947

SPIE.

Event: SPIE Astronomical Telescopes + Instrumentation, 2018, Austin, Texas, United States

Surveying the Epsilon Eridani system Using MagAO

Rachel E. Morgan[a], Ewan S. Douglas[a], Kerri L. Cahoy[a], Jared R. Males[b], Katie M. Morzinski[b], and Laird Close[b]

[a]Massachusetts Institute of Technology, 77 Massachusetts Avenue, Cambridge MA, USA
[b]Steward Observatory, University of Arizona, 933 N Cherry Ave, Tucson, AZ, USA

ABSTRACT

The Epsilon Eridani system is a star system $\sim$ 10 ly away predicted to be similar to our solar system, making it a particularly interesting target for exoplanet detection. A Jupiter-like exoplanet has been predicted at 1.88 arcsec using radial velocity techniques,[1] and an outer debris disk has been imaged at 35 - 90 AU with Spitzer and CSO observations.[2] We present a preliminary survey of the inner system using the MagAO instrument with the Magellan Clay telescope in Chile. We apply and evaluate the Karhunen-Loeve Image Projection technique, which estimates the point spread function (PSF) of the central star for high-contrast imaging using Principal Component Analysis (PCA). We perform this analysis by adapting the pyKLIP package, which was developed for analyzing data from the Gemini Planet Imager instrument, to be used with data from the MagAO/VisAO instrument.

Keywords: MagAO, Epsilon Eridani, KLIP

1. INTRODUCTION

Post-processing and adaptive optics techniques have potential to improve high contrast imaging in astronomy. We present a preliminary survey of the inner system around the star Epsilon Eridani using Karhunen-Loeve Image Processing (KLIP) applied to data from the Magellan Adaptive Optics VisAO (MagAO/VisAO) instrument with the Magellan Clay telescope in Chile.

The KLIP algorithm is an image processing technique that uses Principal Component Analysis (PCA) to estimate the Point Spread Function (PSF) of the central star for high-contrast imaging. We apply this algorithm to data collected with the MagAO/VisAO adaptive optics instrument to demonstrate its utility for post-processing data taken with adaptive optics instruments. We adapt the pyKLIP package* developed for the Gemini Planet Imager instrument[3] to work with MagAO data, including adding World Coordinate Systems (WCS) calculations and contrast curve calibration with throughput correction. We present an analysis of the contrast achieved with pyKLIP reduction for various different numbers of Karhunen-Loeve (KL) modes and different Wavefront Error (WFE) cutoffs in order to quantify the performance gain from to post-processing the data. We also seek to lower barriers to performing state-of-the art speckle subtraction on MagAO datasets by contributing to a publicly available codebase.

This analysis uses data from the Magellan Adaptive Optics (MagAO) instrument with the Magellan Clay telescope in Chile. Data was taken with the VisAO science camera with a *z'* filter. 9,661 frames were taken in total from August 30th to 31st, 2017 under non-photometric and windy conditions. This data was taken to survey the inner Epsilon Eridani system with the goal of imaging its dust belt. However, suboptimal observing conditions limited the exposure time and range of angles collected, which affect the results. We use the pyKLIP software package[3] to implement the KLIP algorithm for post-processing of MagAO data, with the goal of acquiring more data in the future and expanding upon this work. Imaging and understanding dust belts around extrasolar systems is important to understanding solar system structure and evolution and how dust belts affect exoplanet direct imaging.

Further author information:
E-mail: remorgan@mit.edu

*pyKLIP package from Wang et al. $< bitbucket.org/pyKLIP/pyklip >$

Adaptive Optics Systems VI, edited by Laird M. Close, Laura Schreiber, Dirk Schmidt, Proc. of SPIE Vol. 10703, 107032M · © 2018 SPIE
CCC code: 0277-786X/18/$18 · doi: 10.1117/12.2313947

2. BACKGROUND

The Magellan Adaptive Optics (MagAO) instrument is an adaptive optics instrument at the Magellan Clay telescope at the Los Campanas Observatory in Chile. The instrument is a 585-degree-of-freedom AO system with a pyramid wavefront sensor and an adaptive secondary mirror.[4] MagAO can be used with two different science cameras simultaneously, VisAO for observing visible wavelengths (with filters from *r'* to *Ys*) and Clio for observing IR wavelengths (with filters from *J* to *M'*).[5] The VisAO instrument offers significant advantages because of the improved detector performance, darker skies, and improved resolution.[6]

Post processing of image data increases sensitivity to faint objects by removing systematic errors. The Karhunen-Loeve Image Projection (KLIP) algorithm is a post-processing technique that uses Principle Component Analysis (PCA) to subtract an empirical model Point Spread Function (PSF) from high contrast images in order to image exoplanets or debris disks. The algorithm takes a set of reference search areas from the images and computes their Karhunen-Loeve transform in order to estimate the target PSF and produce a final image with the target PSF subtracted using a specified number of KL modes.[7]

The KLIP algorithm has been implemented for coronagraphic images from the Gemini Planet Imager (GPI) through a software package called pyKLIP. PyKLIP supports ADI, SDI, and ADI+SDI data from the GPI instrument at the Gemini South telescope in Chile.[3] One of the goals of this work is to adapt the pyKLIP package to run on data from the MagAO instruments. The pyKLIP package has been used with MagAO instruments in the past by Follette et al. in order to analyze spectral-differential $H\alpha$ images.[8] This paper expands on this work to include World Coordinate System (WCS) calculations for planet injection and contrast curve calibration.

The KLIP algorithm is used to study the Epsilon Eridani star system with the MagAO/VisAO data. The Epsilon Eridani system has been studied extensively in the past because of its proximity to Earth and its sun-like properties. Epsilon Eridani has been observed from the ground with the Subaru telescope by Mizuki et al. 2016, achieving contrast of 14.7 mag at 1" separation.[9] The data taken with the VisAO instrument are in *z'*, which is shorter in wavelength than the Subaru observations.

The Epsilon Eridani system has a Jupiter-like exoplanet detected through radial velocity observations[101] and an outer Kuiper-belt analog disk has been imaged. An infrared-excess in the Spectral Energy Distribution (SED) has been observed, which Backman et al. have postulated is due to a 4-component ring system with narrow, warm belts close to the star and halo-like ice rings further from the star.[2]

3. APPROACH

This analysis is based on data collected from the Magellan Clay telescope in Chile from August 30th to 31st, 2017. On August 30th, 1,831 frames were taken with an exposure time of 0.283 seconds and non-photometric, low wind conditions with seeing ranging from 0.5" - 0.9". On August 31st, 7,830 total frames were taken with an exposure time of 0.283 seconds and seeing ranging from 0.7" - 1.1". The signal varied widely due to non photometric conditions and multiple magnitudes of extinction due to clouds. Data was taken with a *z'* filter on the VisAO instrument. Due to the suboptimal observing conditions, the data collected have a limited exposure time and range of angles on the sky, which affect the results of the Angular Differential Imaging (ADI) analysis. A summary of the data collected is shown in Table 1.

The data collected is reduced by first generating and subtracting darks, centering the star in each frame, and using the gain to convert frames to electron units. Then, the flux from a ghost reflection satellite spot is used to calibrate the photometry of each frame. The ghost reflection satellite spot flux is calculated by smoothing with a Gaussian and is used to calculate the star flux in each frame based on a calculated ratio of satellite flux to star flux measured from unsaturated frames as reported in Males 2016.[11] The data is then sorted into groups based on cutoff wavefront errors (WFE) of 115 nm RMS, 120 nm RMS, and 130 nm RMS and processed with the KLIP algorithm. Note the RMS WFE is reported with the MagAO/VisAO instrument and is used as a comparative quality metric because it is not calibrated absolutely.

KLIP is implemented by adapting the pyKLIP package to work with ADI data from MagAO/VisAO. This involved updating the WCS calculation and contrast curve calibration with throughput correction. KLIP was run with 1, 10, 20, and 35 KL modes for each group of data. The pyKLIP package includes options to partition

Table 1. Summary of data collected August 30th to 31st, 2017 from the MagAO instrument using the VisAO camera at the Magellan Clay Telescope in the Los Campanas Observatory in Chile. Cutoff Wavefront Errors (WFE) were based on RMS WFE reported by the MagAO instrument and were used as a quality metric. Note the RMS WFE value is not calibrated absolutely so it is used comparatively and not as an exact metric. Total exposure time is the total time for each set of data based on the exposure time of 0.283 seconds for each frame. Range of angles is the range of Position Angles (PAs) reported for each frame for Angular Differential Imaging (ADI). Range of angles is not reported for the full dataset because the full dataset was not processed due to large WFE.

RMS WFE Cutoff	Number of Frames	Total Exposure Time	Range of Angles
< 115 nm	35	9.905 s	5.997°
< 120 nm	2180	10 minutes 16.94 s	6.9304°
< 130 nm	4230	19 minutes 57.09 s	6.9574°
All collected data	9661	45 minutes 34.06 s	N/A

the data into subsections and annuli, but KLIP is implemented without segmenting the data (using 1 subsection and 1 annulus) because the goal was to image a dust belt.

A summary of the data processing is shown in Figure 1. Contrast curves are then calculated for each reduced group of data with the satellite spot masked. The contrast is calculated from student-t statistics based on Mawet et al. 2014 in order to account for small sample statistics. Contrast curve correction is then performed by injecting fake planets into the dataset in order to assess the throughput of the KLIP algorithm and correct the contrast calculation for this factor.

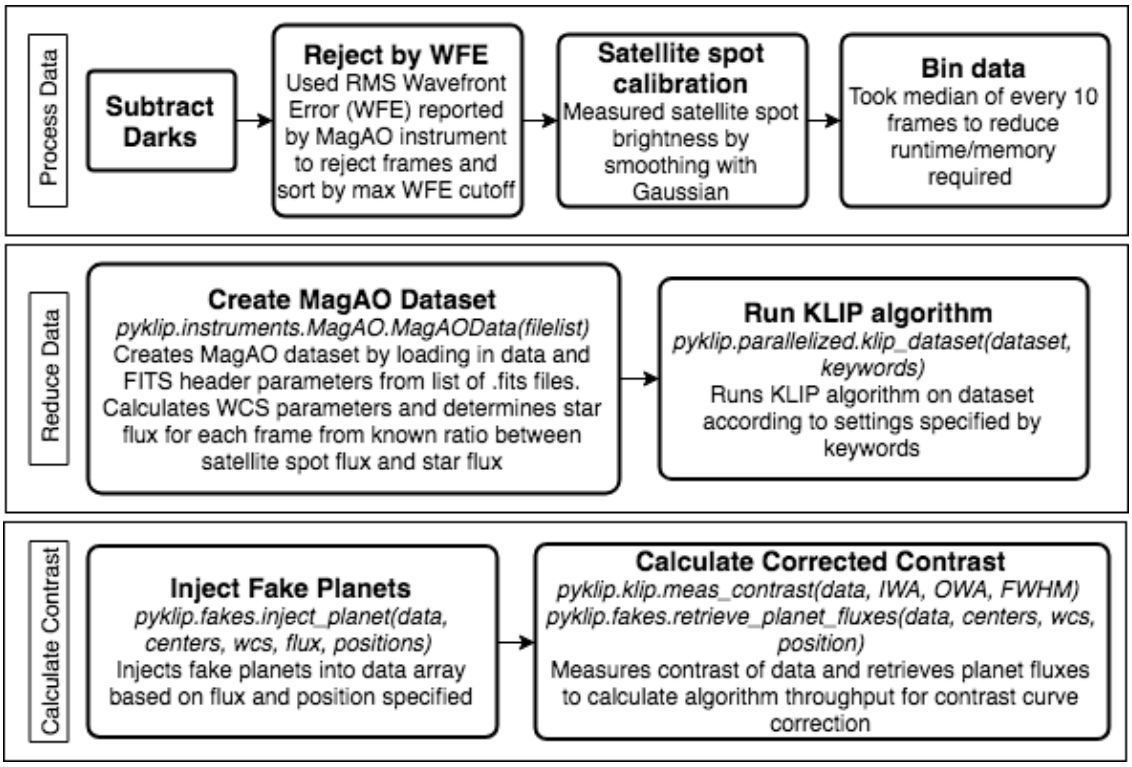

Figure 1. Flow chart of data reduction steps. The first row describes data processing steps prior to the KLIP algorithm, and the second and third rows describe how the pyKLIP package is used to process and analyze the data. The star flux calculation is performed using the known ratio between star flux and satellite spot flux as reported in Males 2016.[4]

The contrast curves are used to determine how contrast was affected by subtracting 1, 10, 20, and 35 KL modes. The contrast results are also used to assess the effect of the cutoff wavefront errors of 115 nm, 120 nm, and 130 nm on the achievable contrast.

4. RESULTS

A representative raw PSF from the MagAO observations is shown in Figure 2. This frame was collected on August 31, 2017 with an exposure time of 0.283 s. The star is saturated in this frame so the star flux is estimated using the ghost satellite spot, which is located to the right of the star, using the ratio between star flux and spot flux from Males 2016.[4] The raw frames run with KLIP with 1, 10, 20, and 35 KL modes.

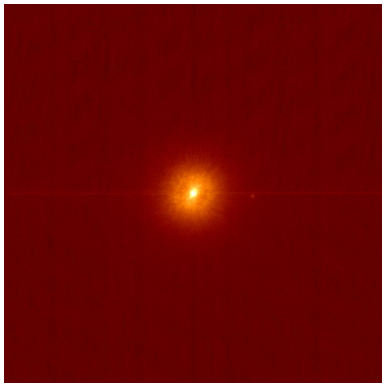

Figure 2. Representative PSF image of Epsilon Eridani collected on August 31, 2017 from the MagAO instrument with the Magellan Clay telescope in the Los Campanas Observatory in Chile. Data was collected with the VisAO science camera with a z' filter and an exposure time of 0.283 s. In this image, the star is saturated so the star flux was calculated using the ghost satellite spot on the right half of the image. This spot is a property of the instrument and has been measured from unsaturated frames so the ratio of the spot flux to star flux from Males 2016[4] can be used to calculate star flux. This figure displays PSF prior to WCS rotation.

Figure 3 shows the results of the KLIP algorithm applied to datasets with WFE cutoffs of 115 nm, 120 nm, and 130 nm with 20 KL modes. KLIP is run with settings of 1 annulus and 1 subsection for these images, but the streaking in each frame led to the apparent quadrants in the output images.

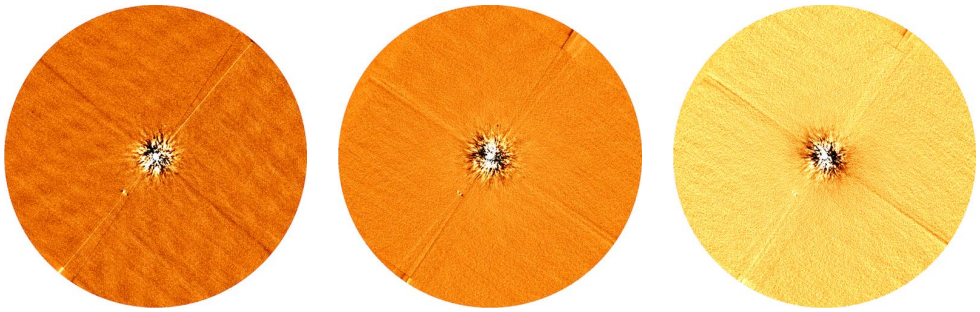

Figure 3. Results of KLIP algorithm applied to each dataset. From left, figures show results for WFE cutoffs of 115 nm, 120 nm, and 130 nm for 20 KL modes. KLIP was applied with 1 annulus and 1 subsection, but streaking in each frame led to the apparent quadrants in the output images. The ghost spot is visible in the lower left corner of each image. These results show how the KLIP algorithm handles data with different levels of WFE and noise.

To calculate the throughput of the algorithm for contrast curve calibration, 16 fake planets are injected into each frame at angles of 10, 100, 190, and 280 degrees for separations of 0.8, 1.2, 1.4, and 1.8 arcsec with contrast levels of 10^{-5} compared to the mean star flux of the dataset. KLIP is then run on the dataset and throughput was calculated as the flux retrieved from each planet in the post-KLIP frame compared to the input flux of the

fake planet. Figure 4 shows a representative image of the 120 nm WFE cutoff dataset with fake planets processed with KLIP with 1 KL mode.

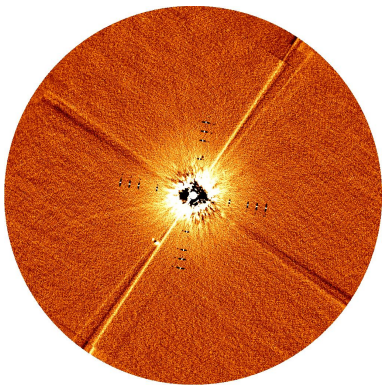

Figure 4. Representative result from KLIP with 1 KL mode from the 120 nm WFE cutoff dataset with 16 fake planets injected. Each planet was injected with a flux of 10^{-5} times the mean star flux for the dataset. The planets appear as the bright spots surrounded by dark sections on either side as the KLIP algorithm over-subtracts around the bright planet. The flux of each planet after KLIP was applied was measured in order to calculate the throughput of the algorithm for contrast curve calibration.

Contrast curves corrected for throughput for each WFE cutoff dataset are shown in Figure 5. The contrast for KLIP applied with each KL mode cutoff is shown compared to the contrast of the mean pre-KLIP frame. The contrast results are not very sensitive to the number of KL modes, but more KL modes led to smoother contrast curves. The number of KL modes had the biggest impact on the largest dataset with cutoff WFE of 130 nm. In this case, subtracting more modes improved the contrast for separations close to the star more than in the other datasets with lower RMS WFE of 115 nm and 120 nm.

Table 2 shows the contrast improvement due to KLIP for each WFE cutoff dataset. The ratio of the mean dataset contrast to the dataset with KLIP applied with 35 KL modes is calculated as an average over all separations and at a representative separation of 1 arcsec. Applying KLIP improved contrast for all WFE cutoff datsets, especially for separations close to the star. KLIP led to the greatest difference in contrast for the largest dataset with a WFE cutoff of 130 nm. In this case, the contrast is improved by almost 15× at a representative close separation of 1 arcsec.

Table 2. Contrast improvement due to KLIP for datasets with RMS WFE of 115 nm, 120 nm, and 130 nm. For each dataset, the mean contrast improvement is the ratio of the mean dataset contrast to the KLIP contrast with 35 KL modes averaged over all separations. The 1 arcsec contrast is the ratio of the mean dataset contrast to the KLIP contrast with 35 KL modes at a representative separation of 1 arcsec. These results show that KLIP offered the largest improvement with the largest dataset with the highest RMS WFE cutoff of 130 nm.

RMS WFE Cutoff	Mean Contrast Improvement (ratio)	1 Arcsec Contrast Improvement (ratio)
< 115 nm	3.07	5.73
< 120 nm	8.19	12.57
< 130 nm	9.27	14.82

Figure 6 shows contrast curves for each dataset with WFE cutoffs of 115 nm, 120 nm, and 130 nm for KLIP applied with 35 KL modes. The smallest dataset with RMS WFE cutoff of 115 nm had the best contrast of $< 10^{-6}$ for separations of $\sim 0.5 - 1$ arcsec. For separations $<\sim 0.5$ arcsec, all datasets had comparable contrast, and past ~ 1 arcsec the 120 nm and 115 nm cutoff sets had comparable contrast which was $\sim 1.5\times$ better than the 130 nm cutoff set. These results imply that the RMS WFE limits the achievable contrast with KLIP

because the larger datasets with longer total exposure time did not improve contrast due to the higher cutoff WFE leading to more noise in the data.

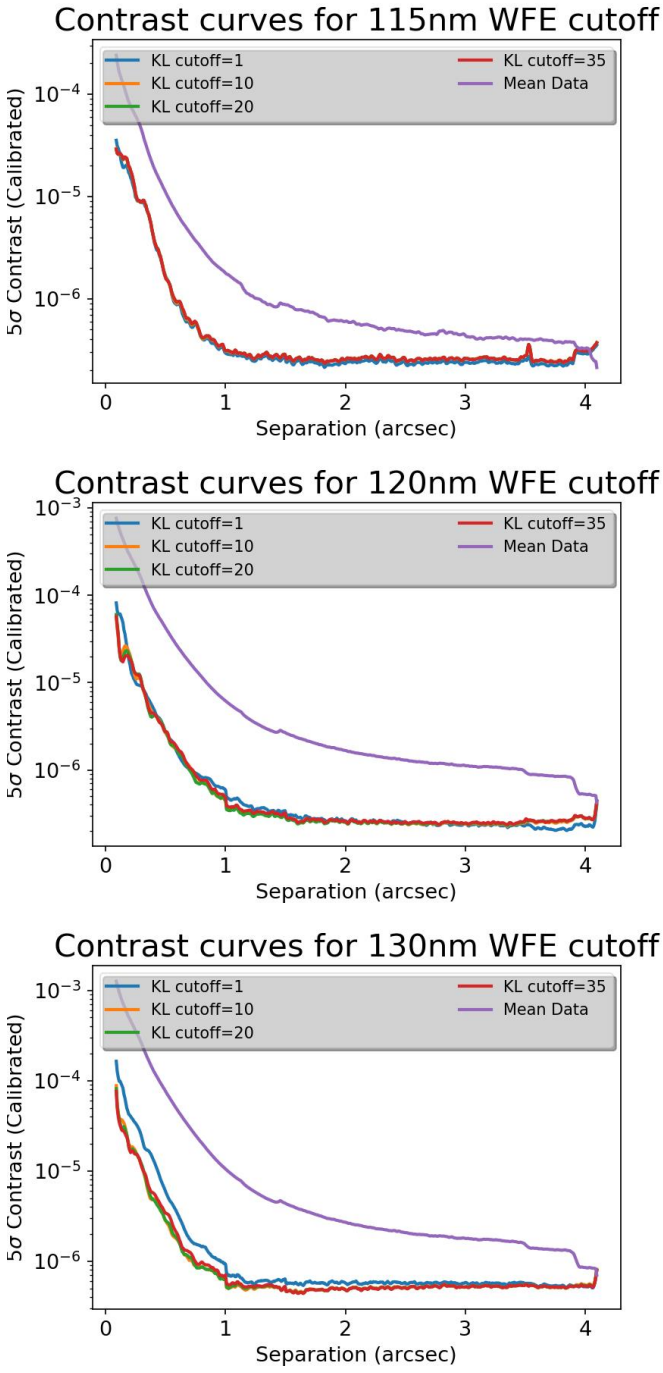

Figure 5. Contrast curves for datasets with WFE cutoffs of 115 nm, 120 nm, and 130 nm (from top). In each figure, results of KLIP with 1, 10, 20, and 35 KL mode cutoffs are shown as well as the contrast of the mean of all frames in the dataset for comparison. These results show that the KLIP algorithm improves contrast compared to the mean of the datasets, and that the number of KL modes subtracted did not affect contrast significantly for the 115 nm and 120 nm WFE cutoff datasets, but that more KL modes did improve contrast of the 130 nm cutoff dataset.

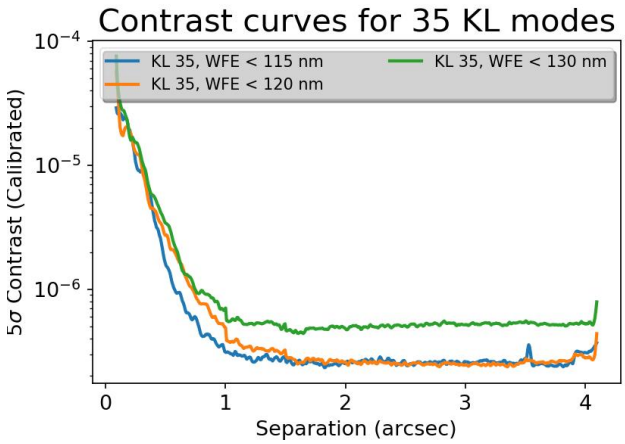

Figure 6. Contrast curve comparing KLIP applied with 35 KL modes from datasets with RMS WFE cutoffs of 115 nm, 120 nm, and 130 nm. Results indicate that larger WFE datasets added more noise and didn't improve the achieved contrast despite the longer total exposure from the larger datasets.

5. CONCLUSIONS

The data presented here is a preliminary survey of the inner Epsilon Eridani system from the MagAO instrument with the Magellan Clay telescope in Chile from August 2017. Non-photometric sky conditions and wind affected the results. However, our analysis with KLIP demonstrates contrast improvement of up to 10-15× compared to the mean data.

This work demonstrates the application of the KLIP algorithm to data collected from the MagAO/VisAO instrument. We update the pyKLIP software package[3] to work with the MagAO/VisAO data by adding WCS calculations and correcting contrast calculations for algorithm throughput by injecting fake planets and computing their post-processed flux. KLIP was run on datasets with RMS WFE cutoffs of 115 nn, 120 nm, and 130 nm with 1, 10, 20, and 35 KL modes. The difference between the mean dataset and the KLIP results are most pronounced for the 130 nm dataset where it leads to a 15× improvement in contrast over the mean dataset. RMS WFE cutoff has a big impact on the achieved contrast, with the 115 nm WFE cutoff dataset having the best contrast of 8×10^{-6} at a separation of 1 arcsec, $\sim 1.5\times$ better than the 130 nm WFE cutoff dataset with KLIP applied with 35 KL modes.

Our results indicate that using KLIP with the MagAO/VisAO instrument data has potential to improve contrast achieved with the instrument. The non-photometric conditions during observations at the telescope limited the total exposure time and the measured angles of data which affected these results. In the future, more data should be taken to improve on these results with KLIP and MagAO/VisAO.

ACKNOWLEDGMENTS

This research was supported by funding from the MIT Undergraduate Research Opportunities Program Thomas Fund, the MIT chapter of the American Association of Aeronautics and Astronautics, and the Massachusetts Space Grant Consortium.

Computation was performed using the MIT Research Computing interface to Massachusetts Green High Performance Computing Center.

KMM's work is supported by the NASA Exoplanets Research Program (XRP) by cooperative agreement NNX16AD44G.

This research made use of community-developed core Python packages, including Astropy,[12] Matplotlib,[13] SciPy,[14] and the IPython Interactive Computing architecture.

The authors would also like to thank Kate Follette and her Amherst College team for their advice and contributions to adapting the PyKLIP package to the MagAO instrument.

REFERENCES

[1] Benedict, G., McArthur, B., Gatewood, G., and et al., "The extrasolar planet ϵ eridani b - orbit and mass," *The Astronomical Journal* **132** (2008).

[2] Backman, D., Marengo, M., Stapelfeldt, K., and et al., "Epsilon eridani's planetary debris disk: Structure and dynamics based on spitzer and caltech submillimeter observations," *The Astrophysical Journal* **690** (December 2008).

[3] Wang, J. J., Ruffio, J.-B., De Rosa, R. J., Aguilar, J., Wolff, S. G., and Pueyo, L., "pyKLIP: PSF Subtraction for Exoplanets and Disks." Astrophysics Source Code Library (June 2015).

[4] Morzinski, K., Close, L., Males, J., and et al., "Direct imaging of beta pictoris b with first-light magellan adaptive optics," *Proceedings IAU Symposium*(299) (2013).

[5] "Information for observers." MagAO Website: https://visao.as.arizona.edu/observers/#parameters. (Accessed: 04 May 2018).

[6] Close, L., Males, J., Follette, K., and et al., "Into the blue: Ao science with magao in the visible," *Proc. SPIE: Astronomical Telescopes and Instrumentation* **9148** (2014).

[7] Soummer, R., Pueyo, L., and Larkin, J., "Detection and characterization of exoplanets and disks using projections on karhunen-loeve eigenimages," *The Astrophysical Journal Letters* (2012).

[8] Follette, K. B., Rameau, J., Dong, R., Pueyo, L., Close, L. M., Duchne, G., Fung, J., Leonard, C., Macintosh, B., Males, J. R., Marois, C., Millar-Blanchaer, M. A., Morzinski, K. M., Mullen, W., Perrin, M., Spiro, E., Wang, J., Ammons, S. M., Bailey, V. P., Barman, T., Bulger, J., Chilcote, J., Cotten, T., Rosa, R. J. D., Doyon, R., Fitzgerald, M. P., Goodsell, S. J., Graham, J. R., Greenbaum, A. Z., Hibon, P., Hung, L.-W., Ingraham, P., Kalas, P., Konopacky, Q., Larkin, J. E., Maire, J., Marchis, F., Metchev, S., Nielsen, E. L., Oppenheimer, R., Palmer, D., Patience, J., Poyneer, L., Rajan, A., Rantakyr, F. T., Savransky, D., Schneider, A. C., Sivaramakrishnan, A., Song, I., Soummer, R., Thomas, S., Vega, D., Wallace, J. K., Ward-Duong, K., Wiktorowicz, S., and Wolff, S., "Complex spiral structure in the hd 100546 transitional disk as revealed by gpi and magao," *The Astronomical Journal* **153**(6), 264 (2017).

[9] Mizuki, T., Yamada, T., Carson, J. C., Kuzuhara, M., Nakagawa, T., Nishikawa, J., Sitko, M. L., Kudo, T., Kusakabe, N., Hashimoto, J., Abe, L., Brander, W., Brandt, T. D., Egner, S., Feldt, M., Goto, M., Grady, C. A., Guyon, O., Hayano, Y., Hayashi, M., Hayashi, S. S., Henning, T., Hodapp, K. W., Ishii, M., Iye, M., Janson, M., Kandori, R., Knapp, G. R., Kwon, J., Matsuo, T., McElwain, M. W., Miyama, S., Morino, J., Moro-Martin, A., Nishimura, T., Pyo, T., Serabyn, E., Suenaga, T., Suto, H., Suzuki, R., Takahashi, Y. H., Takami, M., Takato, N., Terada, H., Thalmann, C., Turner, E. L., Watanabe, M., Wisniewski, J., Takami, H., Usuda, T., and Tamura, M., "High-contrast imaging of epsilon eridani with ground-based instruments," *A&A* **595**, A79 (2016).

[10] Howard, A. W. and Fulton, B. J., "Limits on planetary companions from doppler surveys of nearby stars," *Publications of the Astronomical Society of the Pacific* **128** (2016).

[11] Males, J. R., "VisAO Photometric Calibration," tech. rep., University of Arizona, Steward Observatory (09 2016).

[12] The Astropy Collaboration, Price-Whelan, A. M., Sipőcz, B. M., Günther, H. M., Lim, P. L., Crawford, S. M., Conseil, S., Shupe, D. L., Craig, M. W., Dencheva, N., Ginsburg, A., VanderPlas, J. T., Bradley, L. D., Pérez-Suárez, D., de Val-Borro, M., Aldcroft, T. L., Cruz, K. L., Robitaille, T. P., Tollerud, E. J., Ardelean, C., Babej, T., Bachetti, M., Bakanov, A. V., Bamford, S. P., Barentsen, G., Barmby, P., Baumbach, A., Berry, K. L., Biscani, F., Boquien, M., Bostroem, K. A., Bouma, L. G., Brammer, G. B., Bray, E. M., Breytenbach, H., Buddelmeijer, H., Burke, D. J., Calderone, G., Cano Rodríguez, J. L., Cara, M., Cardoso, J. V. M., Cheedella, S., Copin, Y., Crichton, D., DÁvella, D., Deil, C., Depagne, É., Dietrich, J. P., Donath, A., Droettboom, M., Earl, N., Erben, T., Fabbro, S., Ferreira, L. A., Finethy, T., Fox, R. T., Garrison, L. H., Gibbons, S. L. J., Goldstein, D. A., Gommers, R., Greco, J. P., Greenfield, P., Groener, A. M., Grollier, F., Hagen, A., Hirst, P., Homeier, D., Horton, A. J., Hosseinzadeh, G., Hu, L., Hunkeler, J. S., Ivezić, Ž., Jain, A., Jenness, T., Kanarek, G., Kendrew, S., Kern, N. S., Kerzendorf, W. E., Khvalko, A., King, J., Kirkby, D., Kulkarni, A. M., Kumar, A., Lee, A., Lenz, D., Littlefair, S. P., Ma, Z., Macleod, D. M., Mastropietro, M., McCully, C., Montagnac, S., Morris, B. M., Mueller, M., Mumford, S. J., Muna, D., Murphy, N. A., Nelson, S., Nguyen, G. H., Ninan, J. P., Nöthe, M., Ogaz, S., Oh, S., Parejko, J. K.,

Parley, N., Pascual, S., Patil, R., Patil, A. A., Plunkett, A. L., Prochaska, J. X., Rastogi, T., Reddy Janga, V., Sabater, J., Sakurikar, P., Seifert, M., Sherbert, L. E., Sherwood-Taylor, H., Shih, A. Y., Sick, J., Silbiger, M. T., Singanamalla, S., Singer, L. P., Sladen, P. H., Sooley, K. A., Sornarajah, S., Streicher, O., Teuben, P., Thomas, S. W., Tremblay, G. R., Turner, J. E. H., Terrón, V., van Kerkwijk, M. H., de la Vega, A., Watkins, L. L., Weaver, B. A., Whitmore, J. B., Woillez, J., and Zabalza, V., "The Astropy Project: Building an inclusive, open-science project and status of the v2.0 core package," *ArXiv e-prints* (Jan. 2018).

[13] Hunter, J. D., "Matplotlib: A 2d graphics environment," *Computing In Science & Engineering* **9**(3), 90–95 (2007).

[14] Jones, E., Oliphant, T., Peterson, P., et al., "SciPy: Open source scientific tools for Python," (2001–).